Effect of solid loading and inlet aspect ratio on cyclone efficiency and pressure drop: Experimental study and CFD simulations

Mathieu Morin, Ludovic Raynal, S.B. Reddy Karri, Ray Cocco

Title.
Effect of solid loading and inlet aspect ratio on cyclone efficiency and pressure drop : experimental study and CFD simulations

Authors name and affiliations.
Mathieu Morin[a]
[a] IFP Energies nouvelles, Rond-Point de l'échangeur de Solaize, BP 3, 69360 Solaize, France
mathieu.morin@ifpen.fr

Ludovic Raynal[a]
[a] IFP Energies nouvelles, Rond-Point de l'échangeur de Solaize, BP 3, 69360 Solaize, France
ludovic.raynal@ifpen.fr

S.B. Reddy Karri[b]
[b] Particulate Solid Research, Inc. 4201 W 36th Street, Bldg A, Chicago, IL – USA
reddy.karri@psri.org

Ray Cocco[b]
[b] Particulate Solid Research, Inc. 4201 W 36th Street, Bldg A, Chicago, IL – USA
ray.cocco@psri.org

Corresponding author.
Mathieu Morin
Mathieu.morin@ifpen.fr
IFP Energies nouvelles, Rond-Point de l'échangeur de Solaize, BP 3, 69360 Solaize, France
Phone : +33 (0)437703453

Abstract

This work presents both an experimental and a numerical study on the effect of solid loading and inlet aspect ratio on cyclone performances in a circulating fluidized bed process (CFB). The unit operates at ambient temperature, atmospheric pressure with air and Geldart Group A glass bead particles of median diameter of 42.2 µm. The experimental study investigates the effect of solid loading (i.e. normalized solid loading $C/C_{\max}$ from 0.014 to 0.41) and inlet aspect ratio (from 3 to 7, keeping the inlet area constant) on both gas separation and solid collection efficiencies (fractional and global) and pressure drop. Experimental results showed that cyclone pressure drop is primarily affected by solid loading. This parameter first decreases for normalized loadings up to about 0.127 before increasing for higher values. It was also found that global solid efficiency increases with solid loadings and is strongly favored by

increasing the inlet aspect ratio. The numerical study was carried out with the software Barracuda VR®. It first consists on establishing a methodology on how to simulate cyclones, especially regarding the type of dipleg boundary conditions (BC). The gas flow within the cyclone dipleg, either upward or downward, was found to be a key information for the simulation. For normalized solid loadings up to 0.127, CFD results showed that the gas flows upward in the dipleg with a gas flow rate equal to the loop seal aeration of the CFB while for higher values, the gas flow is downward corresponding to a certain amount of gas underflow. The most appropriate boundary condition to employ in the cyclone dipleg outlet in order to represent the gas flow behavior was found to be a pressure BC whose value leads to either an upward or a downward gas flow. Considering this pressure BC and adapting its value to match the experimental dipleg aeration or gas underflow, the CFD results were found to be in very good agreement compared to experimental data.

Keywords : Cyclone, Solid efficiency, Pressure drop, Experimental study, CFD simulation, Group A particles

1 Introduction

Cyclone separators are widely employed in industries for applications using gas-solid processes [1,2]. The main purpose of this technology is the removal of particles from gases by utilizing the centrifugal force created by the swirling motion of the stream inside the apparatus. According to the type of processes and applications (for instance : Circulating Fluidized Bed processes, Fluid Catalytic Cracking, Biomass and coal gasification…), the gas/solid separator must (i) be as efficient as possible in order to reduce particles emission in the atmosphere and loss of solid out of the process, (ii) be as quickly as possible in order to reduce the residence time in the cyclone and decrease the potential secondary reactions and (iii) minimize the pressure drop across the apparatus [2,3]. The cyclone performances are affected by its geometry and the process operating conditions (i.e. pressure, mass flow rates, gas and solid properties…)

[4]. Among them, both experimental and CFD studies on the effect of inlet aspect ratio and operation at low-to-high solid loadings on cyclone efficiencies and pressure drop was not thoroughly investigated in the literature and are the aim of the present paper. The developed CFD model and methodology may then be applied for developing new technologies which could be commercialized by the FCC Alliance.

A reverse-flow cyclone is generally made of a rectangular inlet duct which tangentially supplies the gas-solid mixture into the cyclone body consisting of a cylindrical barrel with a conical lower end. During the gas solid separation, at a certain axial location of the cyclone body, the swirling gas along the wall reverses itself and flows upward near the cyclone axis before exiting at the top through a vortex finder. On the other side, the particles flow downward along the wall and leave the cyclone at the bottom through a dipleg. Cyclone performances are mainly characterized by its pressure drop and its gas and solid collection efficiency. These two parameters are primordial and can be estimated from either experimental measurements, semi-empirical correlations from the literature or CFD simulations.

1.1 Experimental modeling

Pressure drop in a cyclone can be divided into three main contributions which are influenced by both cyclone geometry and operating conditions [4]:

1) losses at the cyclone inlet which account for inlet contraction and particles acceleration,
2) losses in the separation space which are mainly composed of barrel friction,
3) losses in the vortex finder mainly based on gas-flow reversal and exit contraction.

Cyclones are usually classified as either low-loaded or high-loaded cyclones [5], although the demarcation between the two categories is not well-defined. Most of the works in the literature were conducted for low loading operations, typically less than 1 kg of solid/m^3 of gas [6]. They showed that, for these low-loaded cyclones, the pressure drop decreases by increasing solid loading. This result is due

to the presence of particles near the cyclone wall which increases the frictional resistance to gas flow and then lowers the tangential velocity [7]. For these cyclones, losses from gas-flow reversal dominate the pressure drop. In the case of high-loaded cyclones, Knowlton et al. [5,8] mentioned that the pressure drop increases by increasing solid loading and attributed this effect to solid acceleration losses. They finally associated the demarcation from low- to high- loaded cyclones with this change of pressure drop curve profiles with loading which generally occurs between 1-3 kg_{solid}/m^3_{gas}.

Cyclone pressure drop is usually estimated using the following expression :

$$\Delta P_c = \xi_c \cdot \frac{1}{2} \rho_g U_g^2 \quad (1)$$

where ΔP_c is the cyclone pressure drop (Pa), ρ_g is the gas density (kg/m^3) and U_g is either the inlet or outlet gas velocity (m/s). ξ_c is a dimensionless pressure drop parameter.

In the literature [6,9-14], two types of model are used to represent ξ_c :

- The first method introduces two parameters $\left(\xi_c = \xi_g \times \xi_s\right)$ to account for the effect of cyclone geometry (ξ_g) and solid loading (ξ_s) on cyclone pressure drop. Shepherd and Lapple [9] and Casal and Martinez-Benet [10] considered a dilute flow cyclone and used empirical models to estimate ξ_g. The model takes only into account the effect of geometry through the ratio of inlet to outlet areas. For low-loaded cyclones, ξ_s can be determined using the correlation of Briggs [11]. In the case of FCC particles and various gas inlet velocities, Fassani et al. [15] also showed that the value of ξ_s is approximately constant (equal to 0.5) over a solid loading range up to 20 kg of solid/kg of air, and
- The other method for predicting cyclone pressure drop consists in modeling each pressure loss contribution. For instance, different authors [6,12-14,16,17] represented the dimensionless

pressure drop parameter ξ_c as the sum of inlet acceleration (ξ_{in}), friction with the walls (ξ_{body}) and losses within the vortex core (ξ_{out}). In this case, the model takes into account the effect of solid loading and barrel length on total cyclone pressure drop through friction effects.

Collection or grade efficiency is defined as the fraction of particles of a given size that is retained by the cyclone. Similar to pressure drop modeling, cyclone efficiency was primarily estimated for dilute flow regime in the literature according to three different methods : the "time-of-flight" correlation, the "equilibrium-orbit" model and the "fractional efficiency" approach [4,6,18-20]. The two first models are based on the determination of a critical particle size, d_{50}, also called the "cut diameter". It corresponds to the particle size collected with 50% efficiency and is obtained from forces balance acting on a single particle (i.e. equating the particle mass time acceleration to the centrifugal and drag forces). The smaller the cut diameter, the more efficient the cyclone is. In case of the "time-of-flight" model, the cut diameter is given by the following equation:

$$d_{50} = \sqrt{\frac{9L_w\mu}{\pi N_s \rho_p U_{g,in}}} \tag{2}$$

where L_w is the cyclone inlet width (m), μ is the gas viscosity (Pa.s), $\rho_p$is the particle density (kg/m^3) and N_s is the number of revolutions in the cyclone. Therefore, from Equation (2), the solid efficiency is promoted by decreasing both the inlet width of the cyclone and the gas viscosity and by increasing the inlet velocity, the number of spirals and the particle density.

Once the cut diameter is determined, the collection efficiency η_i of particle diameter d_{pi} can be calculated from :

$$\eta_i = \frac{1}{1 + \left(\frac{d_{50}}{d_{pi}}\right)^m} \tag{3}$$

where m is an exponent generally in the range of 2-6 [6].

The last model (i.e. fractional efficiency model) was developed by Koch and Licht [21,22] and is based on the presence of radial back-mixing of the uncollected particles in the cyclone which is the result of radial drag force, turbulent mixing and particle bouncing into the wall. This approach coupled with the calculation of an average gas residence time in a cyclone gives the following expression for the collection efficiency :

$$\eta_i = 1 - \exp\left\{-2\left[\frac{G\tau_i Q}{D_c^3}(n+1)\right]^{\frac{0.5}{n+1}}\right\} \quad ; \quad \tau_i = \frac{\rho_p d_{pi}^2}{18\mu} \tag{4}$$

where τ_i is the relaxation time (s) of particle diameter d_{pi}, Q is the inlet volume flow rate (m^3/s), D_c is the cyclone diameter (m), G is the cyclone configuration factor which depends on the cyclone design geometry ($G \approx 340 - 700$) and n is the vortex exponent estimated from the relation of Alexander [21].

One limitation of the previous models is that they have been established at low solid loadings. Indeed, the solid collection efficiency is favored when increasing this parameter which is due to very fine particles (i.e. with a size less than 10-20 µm) being trapped in the interstice of larger particles. Several approaches were proposed to account for the effect of solid loading on solid efficiency. For instance, Hoffmann et al. [23] gave the following empirically correlation :

$$\eta = \frac{k_1 c^{k_2} + \eta_0}{k_1 c^{k_2} + 1} \tag{5}$$

where c is the solid loading (kg_{solid}/m^3_{gas}), η_0 is the solid efficiency at zero loading and k_1 and k_2 are constants which can be fitted to experimental data. This equation was successfully applied to predict solid collection efficiency in a horizontal rapid gas-particle separator [24]. Another approach was proposed by Muschelknautz [17] by including the concept of particles sedimentation and critical load.

This method considers that the gas stream can only transport a certain amount of solid at the cyclone inlet (below the critical load) while the other part is mainly separated by sedimentation.

1.2 CFD modeling

Computational Fluid Dynamic (CFD) is increasingly used for developing new processes. Indeed, this powerful tool is applied for simulating different flow configurations (single, two or three phases) including mass and heat transfers and chemical reactions. It can then be employed to complement experimental data, by obtaining information on complex phenomena which are difficult to address experimentally, or for process design, troubleshooting and extrapolation. Consequently, CFD is considered at all steps of process development and for a large number of applications [25].

Cyclone performances may also be predicted using numerical simulations which allow to calculate flow fields of both gas and particles inside the cyclone. According to the particle volume fraction, gas/solid flow can be classified into two different regimes depending on the existence of mutual significant interactions between particles : a dilute or a dense two-phase flow. Generally, two approaches are used to simulate gas/solid flows :

1) In the Euler/Euler approach (EE) also known as two-fluid model (TFM), the gas and the particle phases are described as two interpenetrating continua where the continuity and momentum equations are solved for each phase. The solid phase properties (i.e. granular temperature, solid viscosity, etc) are determined based on the Kinetic Theory of Granular Flow (KTGF) [26]. In the case of cyclone simulations, one limitation of the Euler/Euler model is that a particle size distribution (PSD) of the solid can only be taken into account in the model by adding an additional phase for each class of particle size. This requires solving a new complete set of

balance equations for every additional phase which may be substantially time consuming and causing convergence issues, and

2) In the Euler/Lagrange approach (EL), each particle (or parcel of particles) is tracked individually in a Lagrangian description where the solid motion is defined by classical Newtonian mechanics. The different collisions (i.e. particle-particle and particle-wall collisions) can either be neglected for very dilute flow (one-way and two-way coupling) or be represented for dense flow (four-way coupling) using either the Discrete Element Method (DEM) or the KGTF approach. For instance, in the case of cyclone simulations at very low solid loadings, some authors [27-29] considered a one-way coupling approach which assumes that only the gas phase influences the particle movement. The presence of solid does not affect the gas flow pattern and particle collisions are not represented. For higher but still moderate solid loadings, several researchers [8,30] mentioned that the presence of particles inside the cyclone may (i) attenuate the fluid turbulence and therefore particle dissipation from the wall region to the vortex core, (ii) decrease the strength of the gas swirl and vortex spin rate, (iii) trap very fine particles in the interstices of the larger particles. Consequently, Derksen et al. [30] considered necessary to apply a two-way coupling method which considers that the particulate phase influences the gaseous flow field and vice-versa. However, the non-interacting particles assumption was still retained. Finally, for high solid loadings, the last method (i.e. four-way coupling) accounts for both particle-particle collisions and mutual particle-fluid interactions which can be represented either by the DEM [31] or the KGTF [32]. However, due to its huge requirement of computing time, the four-way coupling approach may be difficult to implement without model modifications.

CFD studies of gas-solid flows at industrial scale imply the simulation of large process geometries containing a significant number of particles. In the case of cyclone simulations, in addition to large size

geometry, high solid loadings at the cyclone inlet may also be needed. In order to simulate processes at industrial scale and overcome the disadvantages of the EE and EL approaches, an alternative Computational Particle Fluid Dynamics (CPFD) method, named Multiphase-Particle-In-Cell (MP-PIC) model, was developed by some authors [33-35]. In this approach, the fluid is modeled as a continuum in the Eulerian framework by solving the Navier-Stokes equations while the solid phase is described using the Multi-Phase-Particle in Cell (MP-PIC) model. The MP-PIC provides a numerical scheme whereby the solid phase is treated as both a continuum and a discrete particle. The particles are grouped into computational parcels or clouds with similar velocities and physical properties (i.e. size, density and species) that are individually tracked. The particle-particle collisions are evaluated by mean of a solid-phase stress. Under these conditions, a complete PSD of the solid phase can be simulated. The MP-PIC approach has been implemented in the commercial code Barracuda VR® which has been used in different studies for simulating industrial scale processes, such as dual fluidized beds [36], Circulating Fluidized Bed (CFB) risers [37], FCC regenerator [38], bubbling fluidized bed [39] and riser termination devices [40].

Regarding the gas phase turbulence model, an adequate description is required to account for the anisotropic turbulent flow inside a cyclone separator. In the literature, two different turbulence models were found to well-predict the gas swirling flow : the Reynolds Stress Model (RSM) [32] and the Large Eddy Simulation (LES) using a subgrid model [41]. For instance, Shalaby et al. [42] performed a comparative study on gas cyclone simulation with the RSM and the LES turbulence models. They reported that the simulation results of LES compare well with experimental data and seem to be the best alternative to conventional turbulence models.

The aim of the present work is to investigate experimentally and numerically the effect of solid loading and inlet aspect ratio on cyclone efficiencies and pressure drop. The cyclone is from a circulating

fluidized bed unit operating at ambient temperature with air and Geldart Group A glass bead particles. The paper is divided into three parts :

1) the experimental setup and numerical method are first introduced,
2) The second part performs a study on the determination of the best boundary condition to employ at the cyclone dipleg outlet for simulating this type of cyclone geometry, and
3) The last sections are dedicated to the comparison between experimental data and CFD results.

2 Experimental section

The experimental tests were performed on a cyclone operating in a circulating fluidized bed unit (CFB) located at Particulate Solid Research, Inc.'s Chicago Research Facility. The schematic diagram of the unit is presented in Figure 1 (A) and consists of a square riser and its associated piping, a bag house filter, the test cyclone and a dipleg/loop-seal arrangement to return solids back into the riser. Several cyclone geometries made of plexiglas were used in this study. A sketch of the cyclone dimensions is shown in Figure 1 (B). It consists of a rectangular, tangential inlet with a height (H) of 323 mm, a width (L_w) of 108 mm and an inlet aspect ratio ($IR=H/L_w$) of 3. The barrel and vortex finder diameter are equal to 430 mm and 190 mm, respectively.

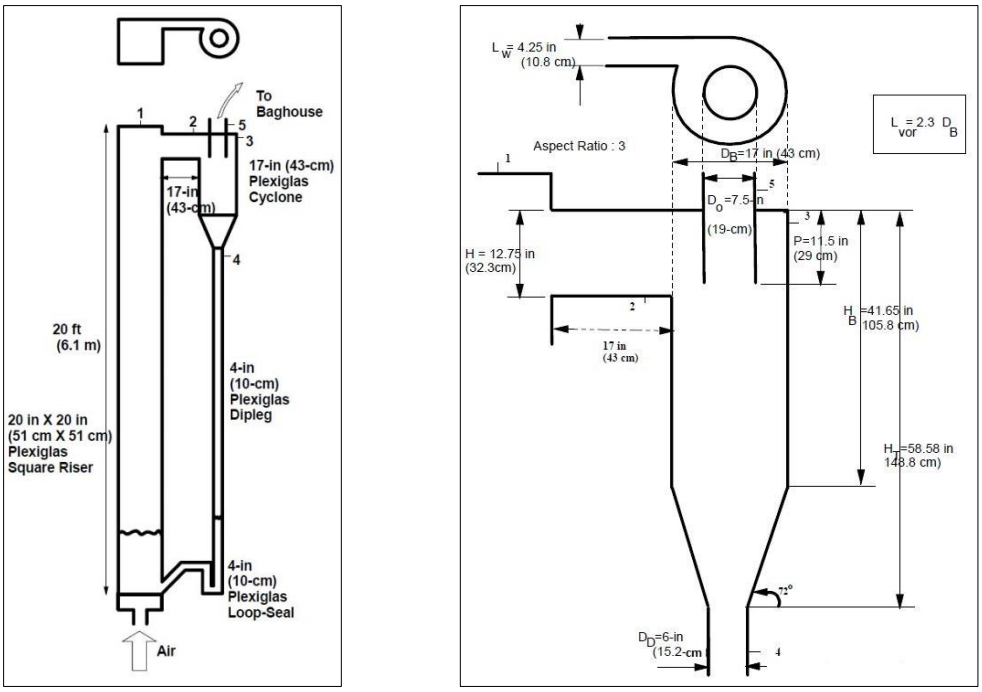

Figure 1 : Experimental setup : (A) Schematic diagram of the square riser/cyclone test unit, (B) schematic drawing and dimensions of the test cyclone with an inlet aspect ratio of 3.

Experiments are performed at ambient temperature and atmospheric pressure. The cyclone is supplied with air at a constant inlet velocity of 15.2 m/s. The solid materials used in this work are Geldart Group A glass beads particles with a medium size ($d_{p,50}$) of 42.2 µm and an apparent density equal to 2402 kg/m^3. In order to limit the presence of electrostatic forces, the entire riser, cyclone, and dipleg are grounded by a winding copper wire. A small amount (5 ppm) level of anti-static agent (Larostat-519) was also added to the powder. The glass beads particle size distribution is presented in **Erreur ! Source du renvoi introuvable.**. The cyclone is fed with a mixture of gas and particles at three different solid loadings which are adjusted by varying the amount of inventory in the CFB. In this article, the solid loadings are normalized with the maximum solid loading acceptable for this cyclone. The three normalized solid loadings are then 0.014 (three replicate experimental tests), 0.127 and 0.407. The separated particles from the cyclone are returned back to the riser through a loop seal which is aerated with air at a constant velocity of 0.15 m/s in the upleg and 0.046 m/s in the downleg. The solid mass flow rate in the

process is measured by closing a valve on the cyclone dipleg and timing the rate at which the level built in the dipleg. Sampling probes are also used to sample particle in the cyclone dipleg. Each experiment was conducted for 2 hours which enables a steady state to be reached. The global and fractional efficiencies were measured by collecting and weighting the fines escaping the cyclone into a bag house filter according to the following expressions :

$$\eta_s = \frac{\dot{m}_{p,\text{dipleg}}}{\dot{m}_{p,\text{dipleg}} + \dot{m}_{p,\text{bag}}} \tag{6}$$

$$\eta_{s,i} = \frac{\text{weight of cut "i"exiting the cyclone}}{\text{weight of cut "i"collected by the cyclone}} \tag{7}$$

where $\dot{m}_{p,\text{dipleg}}$ and $\dot{m}_{p,\text{bag}}$ are the solid mass flow rates in the dipleg and in the bag house, respectively. The weights of cut “i” (having an average diameter $d_{p,i}$) exiting and collected by the cyclone are obtained by measuring the solid mass flow rate and particle size distribution both in the dipleg and in the baghouse. The cyclone pressure drop was measured from the pressure difference between the cyclone inlet and cyclone top outlet.

Two different cyclone parameters were varied in the experimental test program :

- A cyclone inlet aspect ratio (IR) of 3, 5 and 7. This parameter was modified while keeping the inlet rectangular area approximately constant. The following dimensions are then used : ($IR = 3, H = 323$ mm and $L_w = 108$ mm), ($IR = 5, H = 418$ mm and $L_w = 84$ mm) and ($IR = 7, H = 495$ mm and $L_w = 70$ mm).
- A normalized inlet solid loading of 0.014, 0.127 and 0.407.

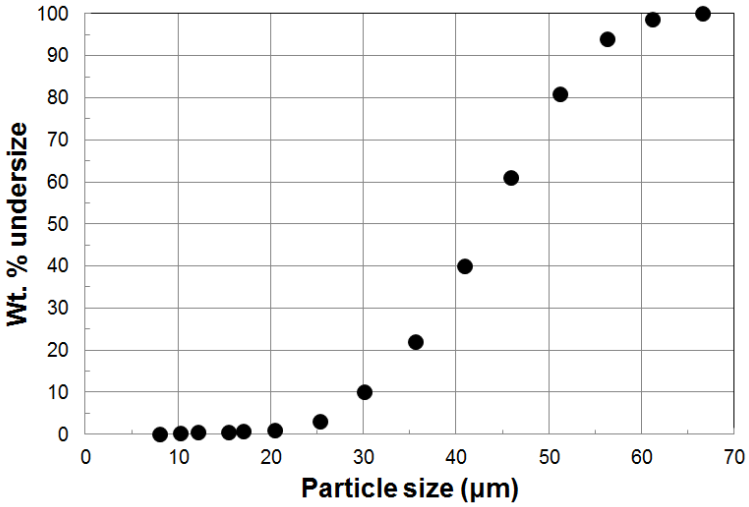

Figure 2 : Particles size distribution of glass beads.

3 CFD method

3.1 CFD model

The CFD model used in this study is from the software Barracuda VR® and is based on the Multi-Phase Particle in Cell (MP-PIC) approach. In this method the gas phase is treated as a continuum in the Eulerian framework by solving the averaged Navier-Stokes equations. The solid phase is grouped into clouds having similar velocities and properties and is treated with a hybrid Eulerian-Lagrangian approach derived from the Liouville equation. Collisions between particles are modeled through a solid stress function. Cohesive forces between particles are not considered. For more details on the solved equations in the MP-PIC method, the reader is referred to the papers of Andrews and O'Rourke [33] and Snider [34,35].

The different simulation parameters used in Barracuda VR® for this study are presented in Table 1. The gas phase is compressible with the ideal gas law used for calculating the density. The turbulence is computed through a Large Eddy Simulation (LES) approach. The large eddies are calculated from the gas

flow equations while the small scale flow structures are captured with the Smagorinsky subgrid scale model (SGS) [43]. Regarding gas interactions with the wall, a no slip condition is applied. The particle-to-wall collisions are computed by means of retention coefficients. A value of 0.85 (default value in the software) is considered for both normal and tangential collisions which indicates that a particle keeps 85% of its normal and tangential velocity after wall collision. The particle normal stress model used in this study is an extension of the model developed by Harris and Crighton [44] with coefficient values recommended by the software. A close packed volume fraction of $\varepsilon_{cp} = 0.55$ is indicated in order to avoid having local dense packed phase zones in the cyclone which are not representative. However, in the case of simulations with a fluidized bed, a value equal to 0.63 was used for the fluidization. Finally, the complete particle size distribution given in **Erreur ! Source du renvoi introuvable.** is applied. The simulation time was fixed to 60 s and a pseudo steady state was reached after 15 s of simulation time. This last value is used for CFD results average.

Table 1 : Simulation parameters.

Model	
Drag law	Wen &Yu/Ergun
Turbulence model	LES with subgrid scale (SGS) model
Particle and gas wall interactions	
Gas to wall interaction	No slip
Particle normal-to-wall retention coefficient	0.85
Particle tangent-to-wall retention coefficient	0.85
Particle-to-particle interaction :	$\tau_s = \frac{10 P_s \varepsilon_p^{\beta}}{\max[\varepsilon_{cp} - \varepsilon_p,\ \alpha(1-\varepsilon_p)]}$
Close-pack volume fraction (ε_{cp})	0.55
Maximum momentum redirection from collision	40%
Pressure constant (P_S)	1 Pa
Non-dimensional constant (β)	3
Non-dimensional constant (α)	10^{-8}
Time setting	
$CFL = u_g \Delta t / \Delta x_{cell}$	$0{,}8 < CFL < 1{,}5$
Simulation time	60 s
Start time for average	15 s

3.2 Numerical setup

3.2.1 Geometry and boundary conditions

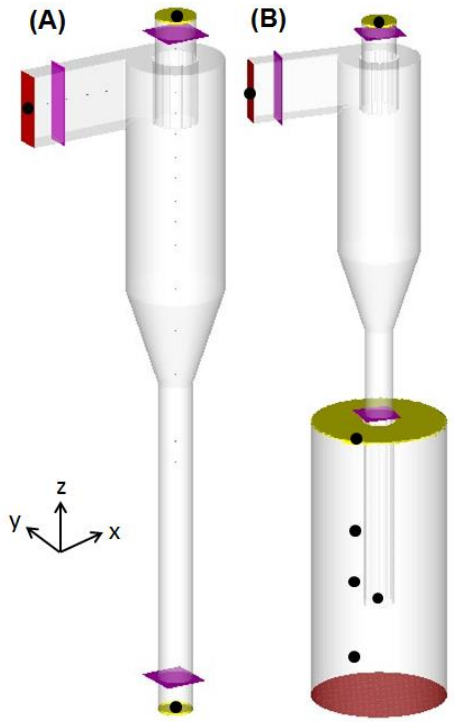

The cyclone geometry used for the simulation is presented in Figure 3 (A). Its dimensions are similar to the ones given in Figure 1. A dipleg length of 1.5 m was employed and was assumed to be long enough to minimize the effect of dipleg BC on the cyclone hydrodynamic. Initially the cyclone is free of particles. The boundary conditions are set in order to fit the different operating conditions. At the cyclone inlet, a constant gas mass flow rate is fixed which corresponds to an inlet velocity of 15.2 m/s while the particle mass flow rate is defined with the desired solid loading. An atmospheric pressure BC is fixed to the top cyclone outlet. Finally, three different dipleg BC were thoroughly studied in this work which are related to the value of the experimental air aeration in the downleg of the loop seal and the solid flux in the cyclone dipleg :

1) A fixed upward air mass flow rate corresponding to an air velocity of 0.046 m/s (i.e. value of air aeration in the downleg of the loop seal).

2) A pressure BC whose value is adapted during the simulation to obtain an average upward air velocity of about 0.046 m/s.
3) An immersed dipleg within a fluidized bed was also tested as potential additional BC. In this case, a fluidized bed of 0.7 m of diameter and 1.5 m of height containing 327 kg of particles is added to the geometry (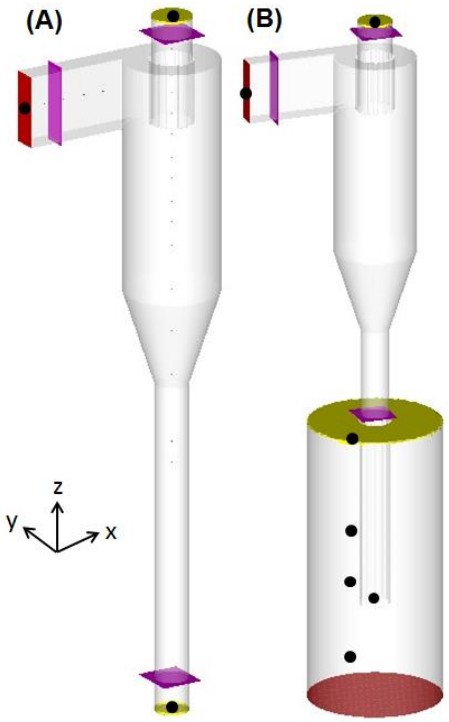

Figure 3 (B)). The geometry values of the fluidized bed have been arbitrary chosen and are assumed to have a small effect on the simulation. The bed is fluidized with an air velocity of 0.2 m/s and the pressure BC at the fluidized bed outlet is adapted to obtain an average air velocity of 0.046 m/s in the dipleg.
4)

Therefore, for these three approaches, it is first assumed that the entire gas flow in the downleg is going upward.

During the simulation, both particle and gas mass flow rates crossing a given section are recorded using different flux planes at the cyclone inlet, top outlet and dipleg ; they are shown as pink rectangles in

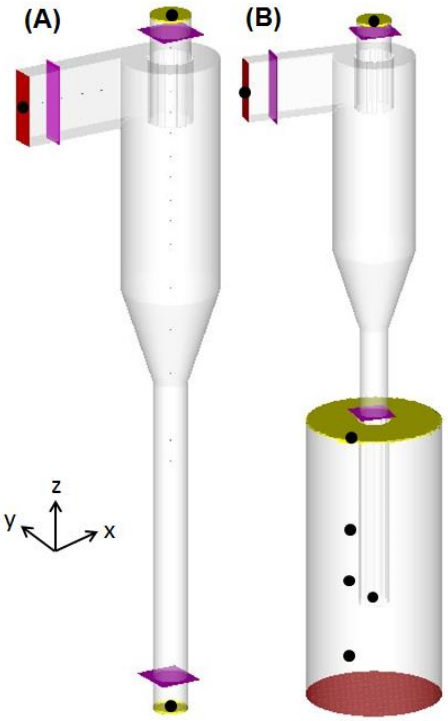

Figure 3. Pressures inside the cyclone are computed at several locations (black dot in

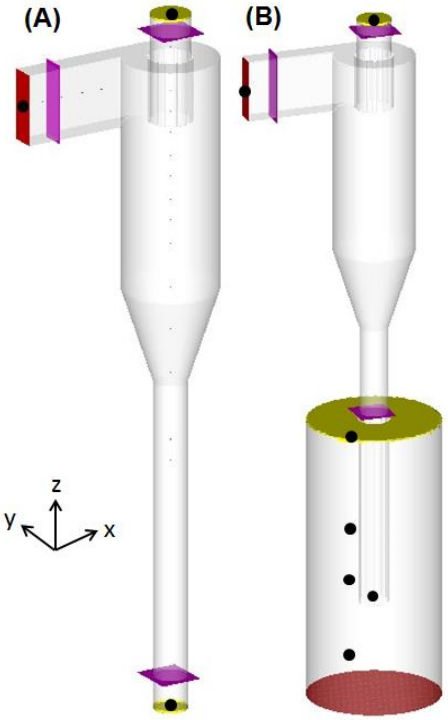

Figure 3). In the following, the cyclone pressure drop corresponds to the pressure difference between the cyclone inlet and top outlet and the solid efficiencies are calculated from Equations (6) and (7).

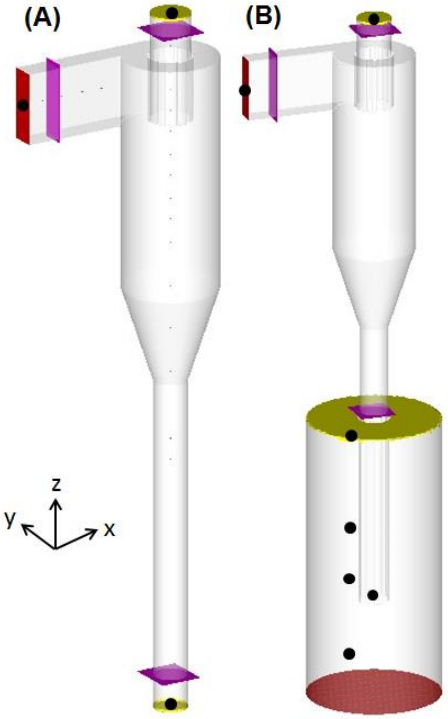

Figure 3 : Cyclone geometry, boundary conditions (red and yellow), flux planes (pink) and computed pressures (black) used for the simulation, (A) BC in the dipleg outlet, (B) dipleg immersed within a fluidized bed.

3.2.2 Mesh

Three different uniform and structured grid resolutions were tested for the simulation, which have respectively 500k, 700k and 1M cubic cells. During these simulations, a constant number density manual was specified at the inlet boundary which indicates that increasing the mesh resolution will scale-up proportionally the particle count in the entire domain. Besides, it was also verified that the simulation was independent of this parameter. The effect of the amount of cells was studied by comparing the average normalized particles flow rate in the cyclone top outlet and dipleg. The results are given in Table 2. It can be seen that the amount of cells in the domain has a strong influence on the particles mass flow rate, especially for solids crossing the cyclone top outlet. For instance, a relative difference of 270% and

2.2% between domain with 500k and 1M cells is found for particles mass flow rates exiting the cyclone top outlet and dipleg, respectively. On the contrary, no difference was observed between the different meshes for pressures and gas mass flow rates through the different flux planes. Therefore, in the following, a cyclone geometry containing 1M cells was used for the simulation and is considered as a good compromise between simulation time and mesh effect.

Table 2: Effect of cells number in the domain on the normalized particle mass flow rate, simulation with a normalized inlet particle loading of 0.127 and an upward velocity of 0.1 cm/s in the dipleg.

Cells	dx × dy × dz	$\dot{m}_{p,\text{top outlet}}/\dot{m}_{p,in}$	$\dot{m}_{p,\text{dipleg}}/\dot{m}_{p,in}$
500 k	$2.7 \times 2.7 \times 2.7$ mm	0.02333	0.9696
700 k	$2.5 \times 2.5 \times 2.5$ mm	0.008636	0.9858
1M	$2.1 \times 2.1 \times 2.1$ mm	0.006363	0.9919

4 Results & discussion

This section is based on two parts. First, a focus is made on the different boundary conditions which can be set in the cyclone dipleg. They have been briefly presented in section 3.2.1. The most appropriate one is selected to perform the CFD simulations. The numerical results are then compared to experimental data by studying the effect of solid loading and inlet aspect ratio on cyclone efficiencies and pressure drop.

4.1 Effect of dipleg boundary conditions

In order to highlight the effect of boundary conditions in the cyclone dipleg, three different modeling approaches were conducted for a normalized solid loading of 0.127 and an IR of 3.

1) The first approach considers a constant upward air mass flow rate in the cyclone dipleg corresponding to an average velocity of 0.046 m/s. The CFD results are presented in

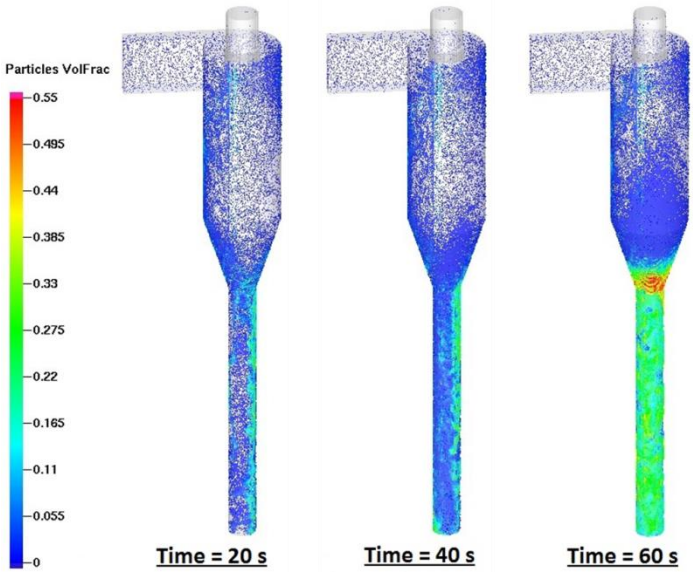

2) Figure 4. It can be seen that the cyclone dipleg progressively floods during the simulation. This dipleg flooding may be a consequence of an overestimation of the drag force. Indeed, imposing a flow BC in the dipleg forces a uniform upward gas flow rate on the lowest horizontal layer of computational cells. If the drag force is overestimated, this leads to a condition where the entire lowest layer is almost free of particles which are suspended just above. As a consequence, only few particles can escape out the domain through the bottom dipleg. This drag force overestimation was observed in several works in the literature, especially during simulations of gas-solid flow with Geldart Group A particles [37,45]. The phenomenon can be explained by (i) experimentally, the presence of inter-particle forces which leads to the formation of clusters with higher diameters than the particle and decreases the drag force. These clusters are not taken into account in the drag force model of Wen & Yu/Ergun and (ii) numerically, mesh size effects which are not able to resolve the fine structures of the flow. Therefore, these observations led some authors to adapt the drag law model in order to better represent the hydrodynamic of Geldart Group A particles. For instance, Gao et al. [45] took into account

particle agglomeration effects in the dense phase of a turbulent fluidized bed by including a cluster diameter in the drag force modeling. In the present study, some simulations were performed by correcting the correlation of Wen & Yu/Ergun [46] with a factor less than 1 in order to account for overestimation of the drag force commonly observed during simulation of Geldart Group A particles. No significant improvements were found and particles still hold up in the dipleg after 50 s of simulation. It can thus be concluded that imposing an upward mass flow rate as boundary condition in the dipleg outlet does not represent the gas-solid flow behavior and was then not used in this study.

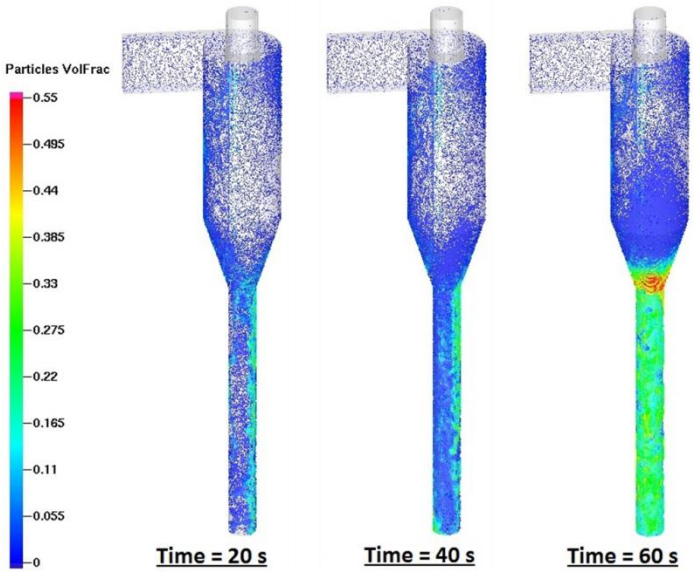

Figure 4 : Cloud volume fraction for different simulation times, simulation with a constant upward gas mass flow rate in the dipleg corresponding to an average velocity of 0.046 m/s.

3) The second approach corresponds to a pressure BC set at the outlet of the cyclone dipleg. It was found that this boundary condition strongly influences the flow behavior inside the dipleg and, according to the pressure value, can lead to the presence of either an upward or a downward gas flow. Numerically, a small change in the dipleg pressure BC can indeed yield to a substantial variation in the gas velocity. This result is presented in Table 3. In this table, the gas underflow

represents the percentage of inlet gas flow rate flowing downward in the dipleg. It is also related to gas efficiency with the following equation :

$$\eta_g(\%) = 100 - U \tag{8}$$

where U is the gas underflow (%), $U = \dot{m}_{g,dipleg}/\dot{m}_{g,in}$.

Table 3 : Dipleg pressure BC and the corresponding averaged gas velocity in the cyclone dipleg (negative and positive velocities correspond to downward and upward flows, respectively).

Dipleg pressure BC (Pag)	Ug dipleg (m/s)	Gas underflow (%)
0	-11.5	38
500	-1.57	5.3
548	-0.82	2.7
558	-0.70	2.3
595	+0.3	0

For instance, a constant pressure BC value of 558 Pag leads to an average downward gas velocity of 0.7 m/s over the dipleg section while a constant pressure BC of 595 Pa leads to an average upward gas velocity of 0.3 m/s. For this latter case, it is also important to note that no dipleg flooding was observed. Consequently, to represent the experimental upward gas velocity

aeration within the dipleg (i.e. 0.046 m/s), the pressure BC must be adapted during the simulation.

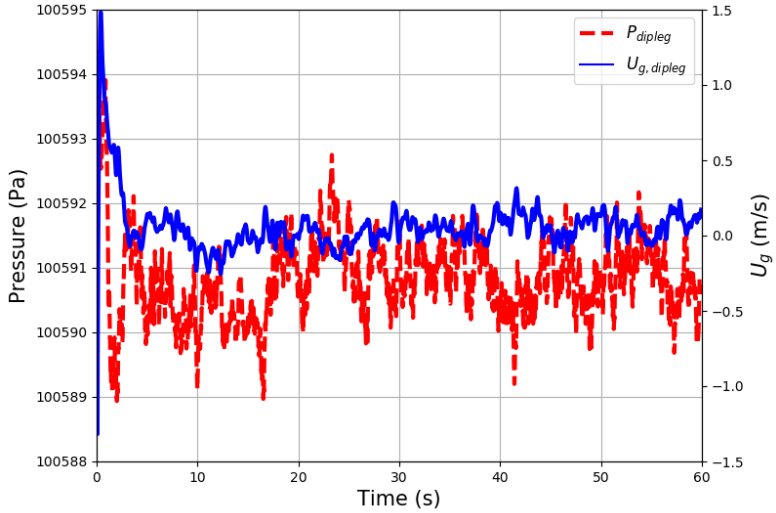

Figure 5 shows the pressure BC value adjusted during the simulation and the corresponding gas velocity in the dipleg. It can be seen that, for simulation times less than 15 s, the pressure BC value was not large enough to lead to an upward gas velocity in the dipleg. Consequently, the value was slightly increased, oscillating between 590 and 592 Pag. For this simulation, the average pressure BC and upward gas velocity values were 590.9 Pag and 0.044 m/s, respectively.

CFD results of cloud volume fraction and average axial particle and gas velocities over the dipleg

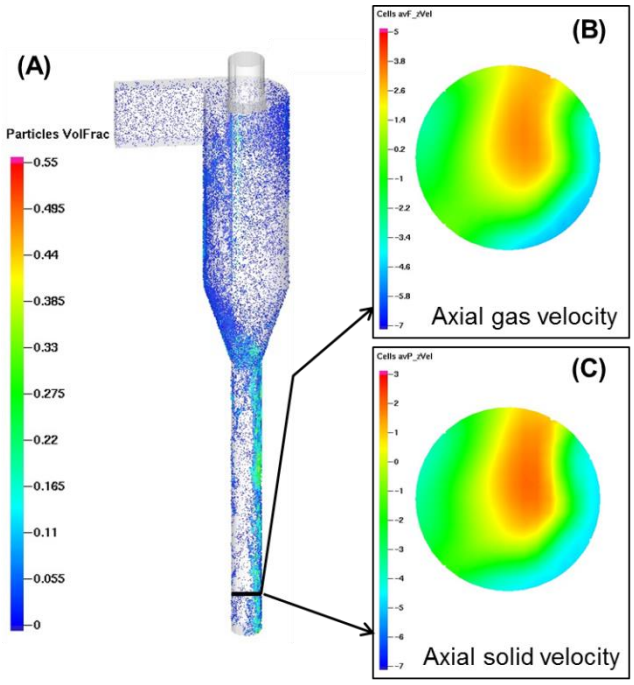

surface are presented in

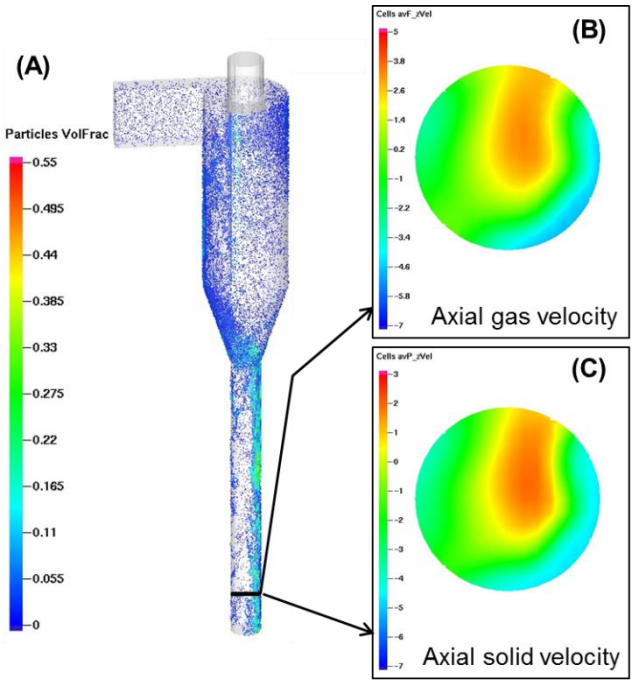

Figure 6. For this type of BC,

Figure 6 (A) shows that the cyclone dipleg does not flood. Besides,

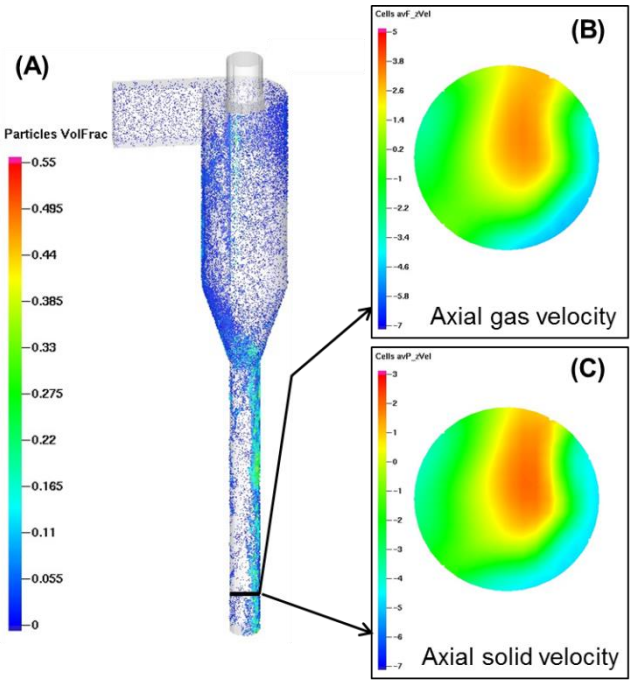

Figure 6 (B) and (C) indicate that the gas and particle flow velocities are not well distributed over the dipleg surface. Particles and gas tend to flow downward near the dipleg wall while upward velocities are rather located near the dipleg center. This BC seems to be a good compromise and will be used in the CFD model for comparison with experimental data.

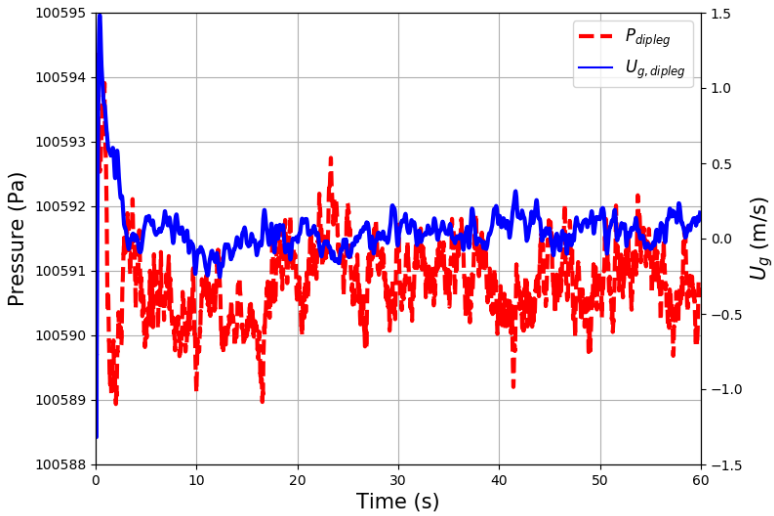

Figure 5 : Dipleg pressure BC and corresponding gas velocity.

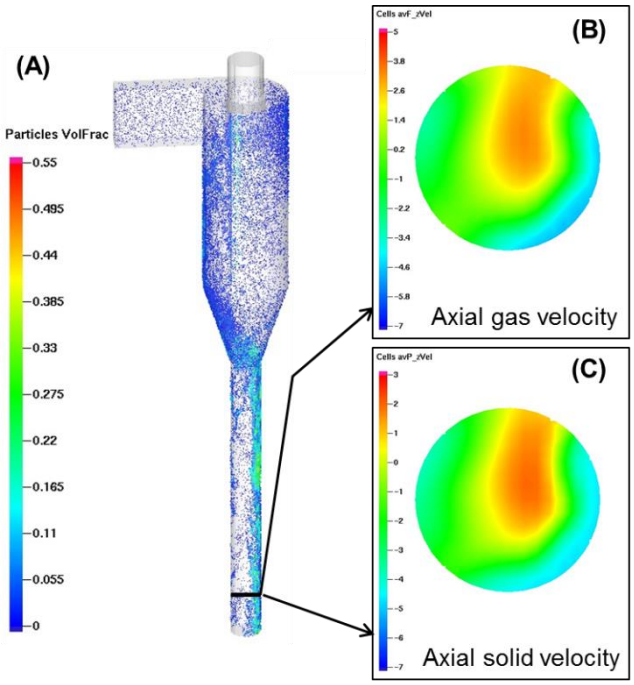

Figure 6 : CFD results for a simulation with a pressure BC in the dipleg adjusted to approach an average upward gas velocity of 0.046 m/s, (A) cloud volume fraction at 60 s of simulation, (B) and (C) average gas and particles axial velocity in the xz-plane.

4) An alternative third approach consists in immersing the cyclone dipleg within a fluidized bed. The

pressure BC is then set to the top of the fluidized bed as shown in

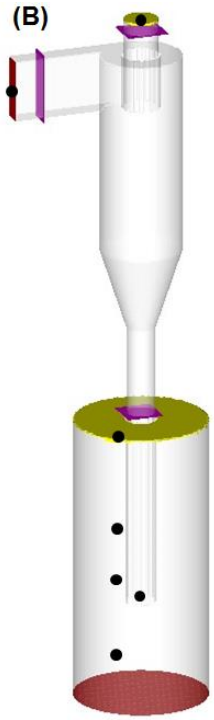

Figure 3 (B) and adjusted during the simulation to obtain the upward gas velocity aeration in the dipleg.

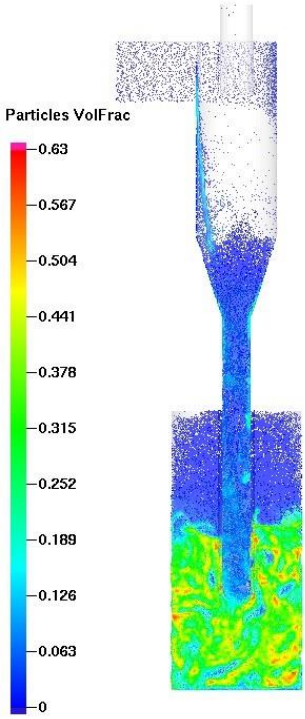

5) Figure 7 presents the results of particle volume fraction in the domain. It can be seen that the dipleg, initially filled of particles to the same level that the bed, empties with a very low particle volume fraction. This phenomenon seems not to represent what would happen experimentally when a cyclone dipleg is immersed in a fluidized bed. Indeed, for both positive and negative cyclones, a dense phase should be established in the dipleg and obey a pressure balance [47]. As the simulation does not represent the dipleg sealing, both gas and solid flow behaviors may not be well-predicted. This type of boundary condition has then not been selected in this work.

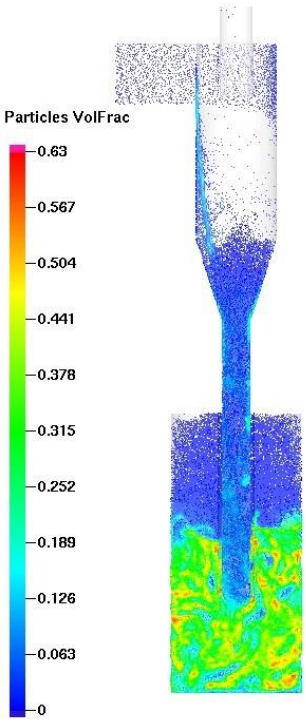

Figure 7 : Cloud volume fraction at 30 s of simulation with the cyclone dipleg immersed within a fluidized bed, IR =3 and a normalized loading of 0.127.

4.2 Effect of solid loading

In the following sections, the effect of solid loading and inlet aspect ratio on cyclone efficiencies and pressure drop is experimentally and numerically discussed. The numerical approach consists in adjusting the pressure boundary condition value in the cyclone dipleg during the simulation in order to approach the desired experimental upward gas flow in the dipleg.

The effect of solid loading on cyclone efficiency and pressure drop was performed for the three different inlet aspect ratios (i.e. $\mathrm{IR} = 3, 5 \text{ and } 7$**).**

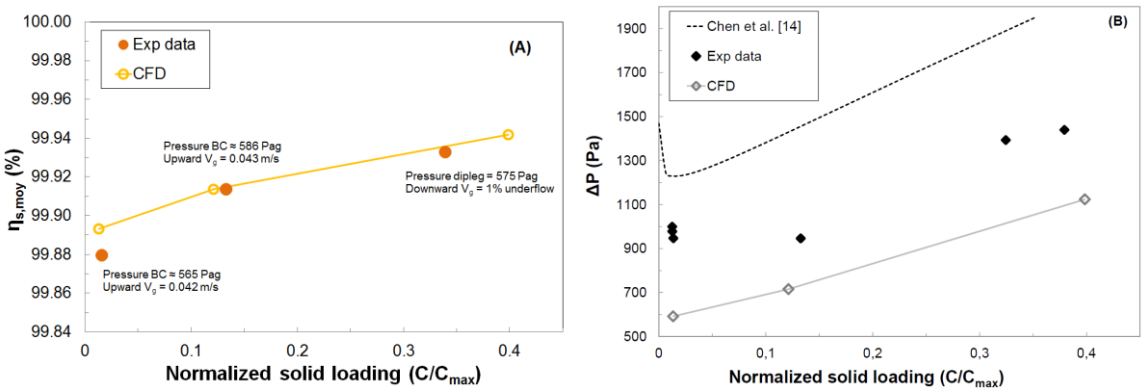

Figure 8 presents the comparison between experimental and CFD results for $\mathrm{IR} = 5$. Several observations can be highlighted :

An increase in the solid loading improves cyclone solid efficiency. This results is well-known in the literature [6,5] and is attributed to higher collection of fine particles which are trapped in the interstices of larger particles.

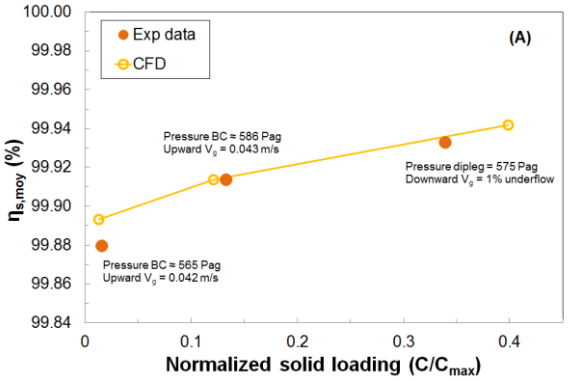

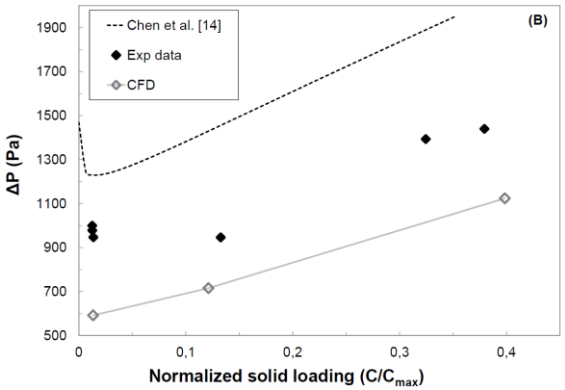

- Figure 8 (A) shows that the solid efficiency is well-estimated by CFD. In the case of normalized solid loadings of 0.014 and 0.127, the gas flows upward in the dipleg and the pressure BC was adjusted during the simulation in order to approach an aeration value of 0.046 m/s. The final

adjusted pressure BC and corresponding gas velocity values averaged from 15 s to 60 s are 565 Pag and 0.042 m/s for a normalized solid loading of 0.014 and 586 Pag and 0.043 m/s for a normalized solid loading of 0.127. For higher normalized solid loadings (i.e. 0.407), it was numerically found that the gas no longer flows upward in the dipleg. Indeed, a simulation with a pressure BC corresponding to an upward gas aeration of 0.045 m/s was performed and led to a substantially lower solid efficiency compared to experimental result (99.45% instead of 99.93%). Karri and Knowlton [48] mentioned that the flow behavior within the dipleg can be related to the solid flux. They reported that for dipleg solid fluxes up to 80 kg/m^2/s, the gas flow is upward while for higher values, the gas flows downward. Consequently, from the works of these authors [48], an estimation of dipleg underflow gives a value of 1-2% for a normalized solid loading of 0.407. The cyclone simulation with a downward gas velocity corresponding to 1% underflow in the dipleg well-represents experimental results for a normalized solid loading of 0.407. Besides, in the case of downward gas velocities in the cyclone dipleg (i.e. high solid loadings), it was found that either imposing a negative gas velocity BC or adapting a pressure BC value during the simulation give similar results. Therefore, for simplification purpose, a negative gas velocity at the dipleg outlet has been selected.

Experimentally, the pressure drop decreases with normalized solid loadings approximately up to about 0.127 and then increases for higher loadings (

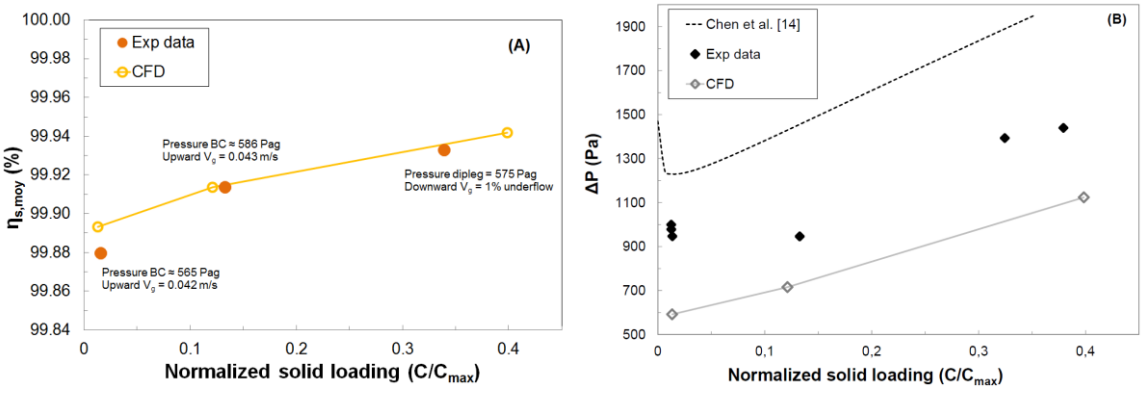

Figure 8 (B)). For low loadings, this phenomenon is due to the presence of solid which decreases the tangential velocity in the cyclone [4]. At higher loadings, the pressure drop due to solids acceleration becomes so large that the cyclone pressure drop increases as solid

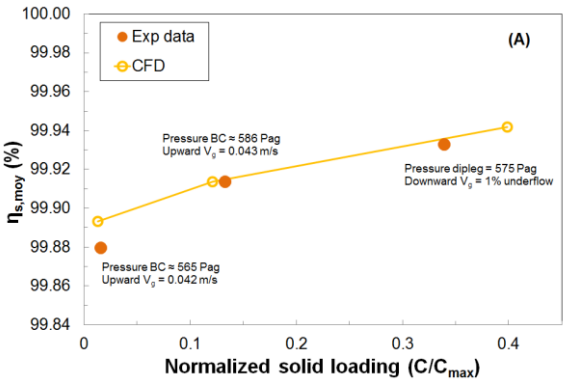

loading increases [8].

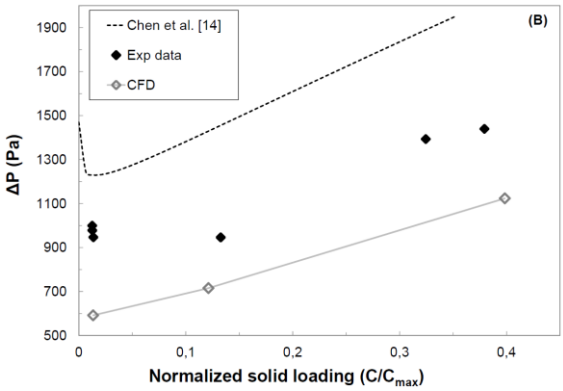

- Figure 8 (B) shows that cyclone pressure drop from CFD results increases with solid loading with a relative difference of about 20-30% with experimental results. The CFD model is not able to capture the experimental ΔP curve profiles. Estimation of pressure drop from the work of Chen et al. [14] is also indicated in the Figure. These correlations are known to be able to predict the ΔP profile with solid loading (i.e. first decrease in pressure drop at low loadings followed by an increase for higher loadings). However, it was found that Chen et al. correlations overestimate (also by a factor of 30%) our experimental data Another estimation of the pressure drop from Equation (1) combined with the relation of Shepherd and Lapple [9] for ξ_g and $\xi_s = 0.5$ gives a constant approximation of cyclone pressure drop ($\Delta P_c = 1085$ Pa) for low to medium loadings while it underestimates it for large loadings.

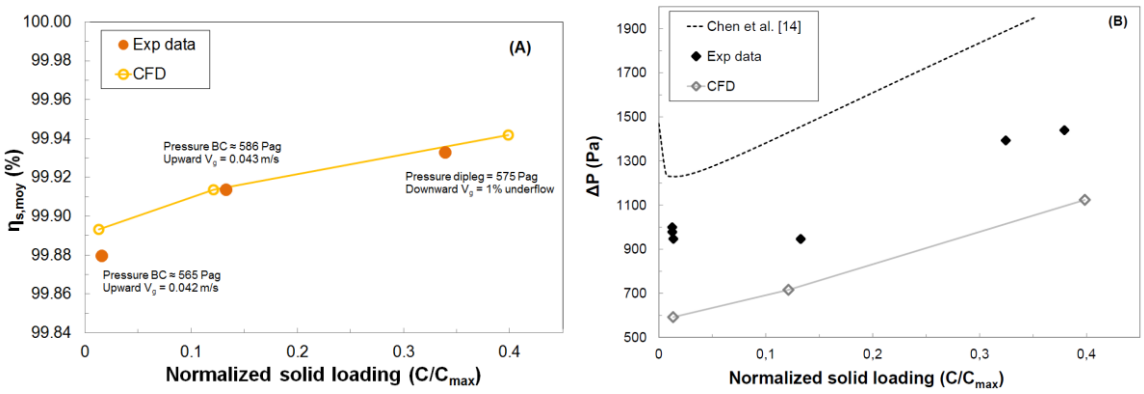

Figure 8 : Effect of solid loading on (A) cyclone efficiency and (B) pressure drop, comparison between experimental and CFD results, IR = 5.

4.3 Effect of inlet aspect ratio

The effect of inlet aspect ratio on solid collection efficiency for different solid loadings is given in

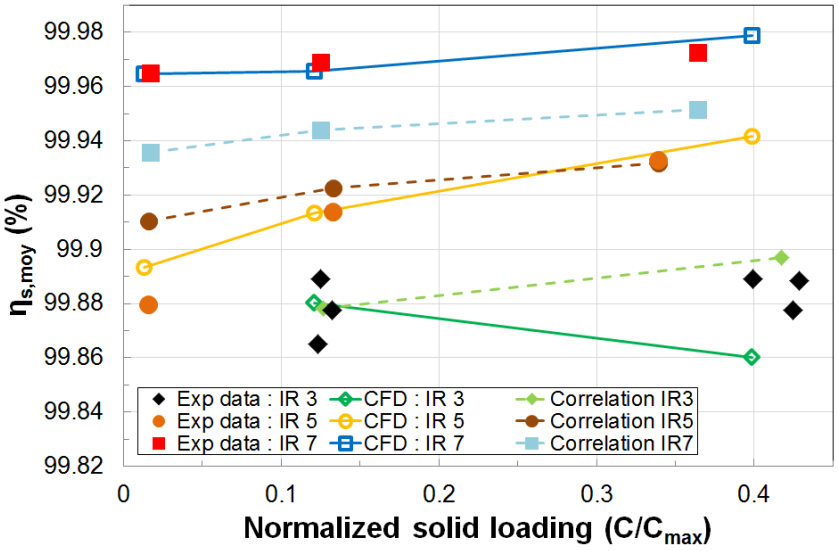

Figure **9**. The different CFD results (i.e. solid efficiency, dipleg pressure and gas velocity) are reported in Table 4. It can be seen that CFD results well-predict cyclone efficiencies for each solid loading and IR. As mentioned in section 4.2, for normalized solid loading up to 0.127 and each inlet aspect ratio, the gas flow in the cyclone dipleg is upward and was simulated by adjusting the pressure BC in the dipleg outlet. The final averaged pressure value is similar for the three IR and a given solid loading. For a normalized solid loading of 0.407, the gas flow is downward corresponding to a certain amount of gas underflow.

This underflow value was found to be in the range of 1-3% and was obtained numerically by imposing a negative gas velocity BC in the cyclone dipleg.

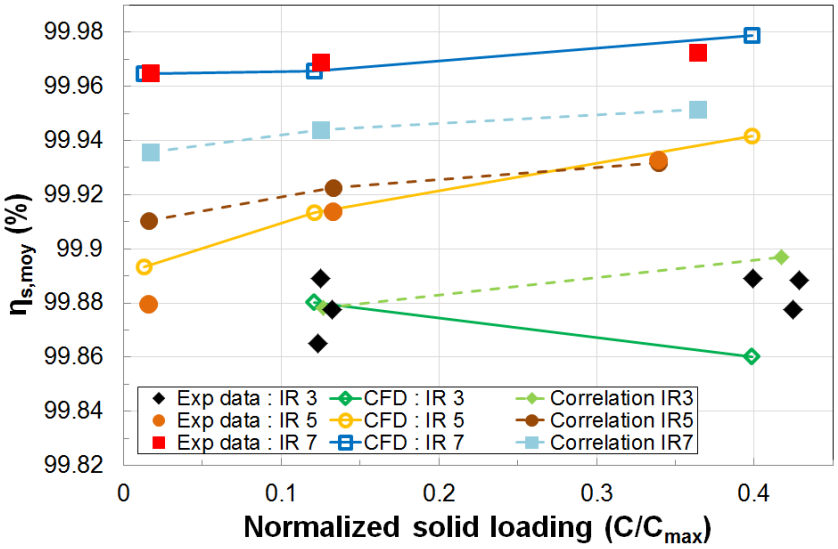

Figure **9** also indicates the solid efficiency results calculated from Equations (2), (3) and (5) by fitting parameters m, k_1 and k_2 ($m = 3.67, k_1 = 0.166$ and $k_2 = 0.558$). A satisfactory global estimation is obtained for IR of 3 and 5 and each solid loading. However, the correlation seems to underestimate experimental results for an inlet ratio of 7. This difference could be explained by parameter m in Equation (3) which, in

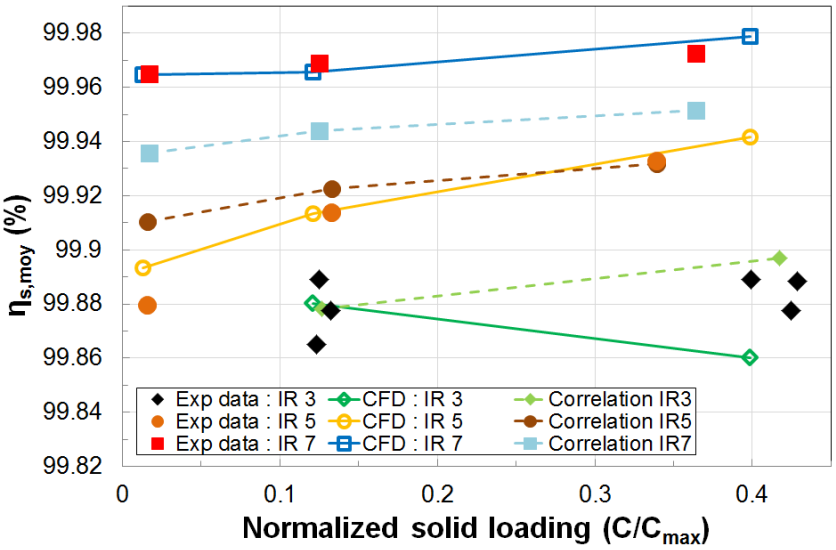

Figure **9**, has the same value for each IR whereas it may be dependent on cyclone geometry.

Regarding cyclone pressure drop, experimental and CFD results showed that the inlet aspect ratio has no effect on this parameter.

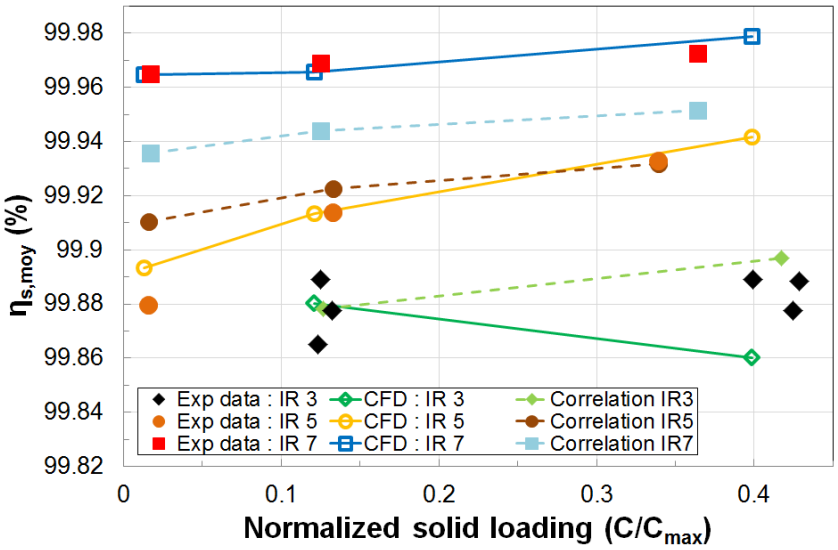

Figure 9 : Effect of solid loading for various inlet aspect ratios on solid efficiency, comparison between experimental data and numerical results.

Table 4 : CFD results for solid efficiency, average pressure BC and gas velocity in the dipleg for different loadings and aspect ratios.

	Normalized solid loading (C/C_{max})								
	0.014			0.127			0.407		
Inlet aspect ratio	η_s (%)	P_{dipleg} (Pag)	$U_{g,dipleg}$ (m/s)	η_s (%)	P_{dipleg} (Pag)	$U_{g,dipleg}$ (m/s)	η_s (%)	P_{dipleg} (Pag)	Underflow (%)
3	-	-	-	99.880	591	0.044	99.860	581	3
5	99.893	565	0.042	99.913	586	0.043	99.942	575	1
7	99.965	554	0.044	99.966	589	0.049	99.978	551	2

4.4 Fractional efficiency

During experiments, measurement of the particles size distribution of the non-collected particles at the cyclone top outlet is performed and the fractional efficiency is calculated from Equation (7). For two different inlet aspect ratios ($IR = 3 \text{ and } 7$) and a given normalized solid loading of 0.407, the

fractional efficiency is plotted versus particle diameter in

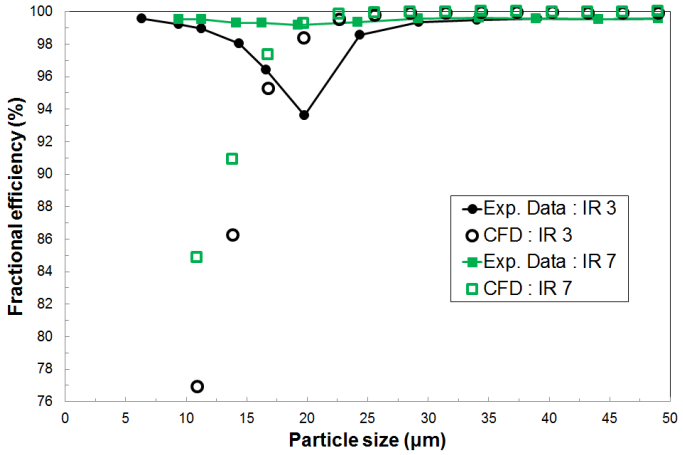

Figure 10. This result gives information on which particle size is well-collected by the cyclone.

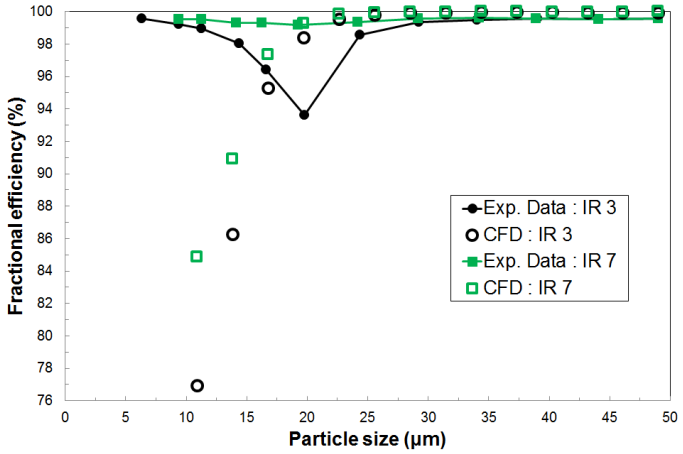

Figure 10 shows that, experimentally, the fractional efficiency decreases with decreasing particle sizes down to 20 µm and then increases for lower particle sizes. This curve trend is associated with the formation of clusters (agglomerated particles) for particles size less than 20 µm which is mainly due to the presence of inter-particle forces. These clusters have larger diameters and are easier to collect by the cyclone. The fractional efficiency is also higher by increasing the inlet aspect ratio.

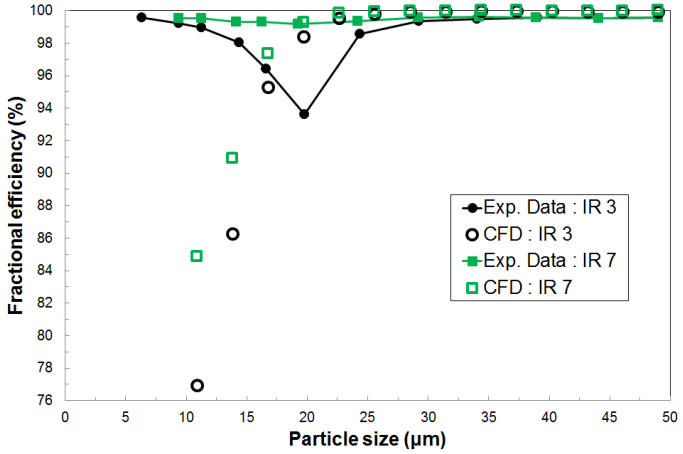

Figure 10 also illustrates fractional efficiency from CFD results. As no models have been used for particles agglomeration, the fractional efficiency increases with particles diameter. It is important to note that the

default agglomeration model available in Barracuda VR® was not able to represent experimental curve profiles in Figure 10.

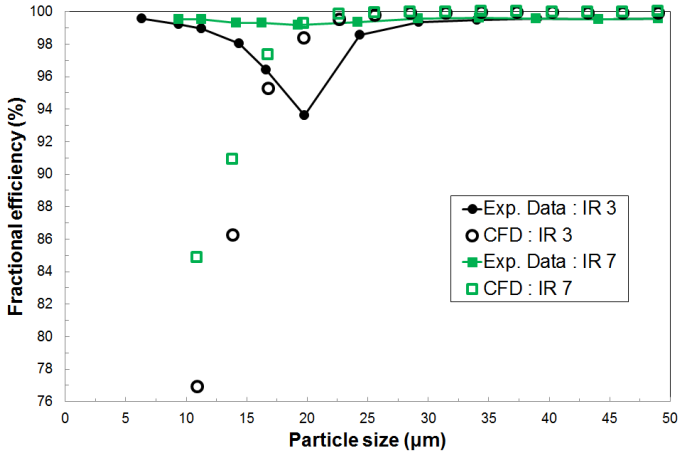

Figure 10 : Comparison between experimental and numerical fractional efficiencies for IR = 3 and 7 and a normalized solid loading of 0.407.

4.5 Effect of gas underflow at high solid loadings

The effect of gas underflow on solid efficiency for two inlet aspect ratios of 3 and 7 and a normalized solid loading of 0.407 is given in Figure 11. These various gas underflows were obtained by imposing a negative gas velocity in the dipleg for the different simulations. This figure shows that the solid efficiency is strongly influenced by the underflow. A higher gas underflow (i.e. a lower gas efficiency) tends to carry particles downward and then promotes the solid to be collected by the cyclone. Besides, Knowlton [48] reported that the higher the solid flux in the cyclone dipleg, the larger the gas underflow. Therefore, a higher solid collection efficiency leads the particles to carry gas downward and then favors the underflow.

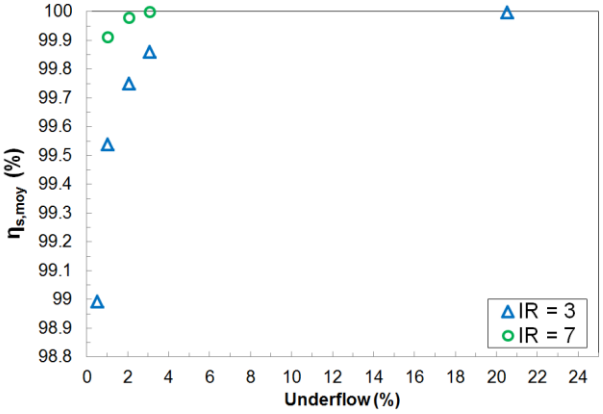

In numerical simulations of cyclones at high loadings, information regarding either gas underflow or gas efficiency must then be known or at least estimated in order to well-predict the solid collection efficiency by CFD.

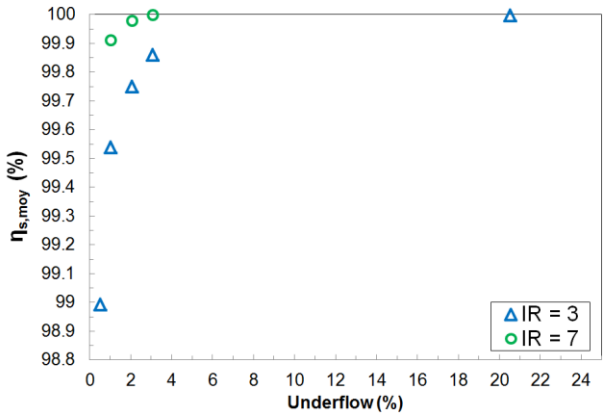

Figure 11 : Effect of gas underflow on solid collection efficiency for a normalized solid loading of 0.407 and two IR of 3 and 7.

5 Conclusions & perspectives

This paper presented both experimental and CFD results on cyclone performance from a circulating fluidized bed process. The unit operates at ambient temperature, atmospheric pressure, with air and Geldart Group A glass bead particles of medium diameter of 42.2 µm. Experimentally, the effect of solid loading (normalized values from 0.014 to 0.407) and inlet aspect ratio (IR = 3, 5 and 7) on the cyclone solid collection efficiencies (global and fractional efficiencies) and pressure drop have been particularly studied. The CFD study was carried out with the software CPFD Barracuda VR® and was first based on establishing a methodology on how to simulate this kind of cyclones, especially regarding the type of boundary conditions to employ. The CFD results were then compared to experimental data and the effect of gas efficiency on the cyclone behavior was also considered.

From the experimental study, the following observations have been highlighted :

- the cyclone pressure drop first decreases with normalized solid loadings up to approximately 0.127 before increasing for higher values. Besides, changing the inlet aspect ratio while keeping the inlet area constant has no effect on this parameter.
- The global solid collection efficiency increases with solid loading. This effect is associated with the higher collection of fine particles which are trapped in the interstices of larger particles. Moreover, the higher the inlet aspect ratio, the higher the solid collection efficiency.
- The fractional collection efficiency was found to decrease with decreasing of particles size down to 20 µm and then to increase for lower particle sizes. This curve trend was attributed to the formation of clusters (agglomerated particles) for particles size less than 20 µm which are easier to collect for the cyclone.

From the different CFD approaches tested, it was underlined that a pressure BC at the dipleg outlet is the best way for simulating these types of cyclone. The crucial information to determine is the gas flow behavior within the dipleg. Numerically, according to the pressure BC value, the gas flows either upward or downward in the cyclone dipleg. It was found that, for normalized loadings up to 0.127, the gas flows upward with a flow rate equal to the loop seal aeration while for higher values the gas flow is downward. The pressure BC was then adapted during the simulation to represent the gas flow behavior and the CFD results showed a very good agreement with experimental data.

Finally, it was also highlighted that, for high loadings, two linked phenomena occur and affect the solid efficiency :

- The CFD results showed that the solid collection efficiency is strongly influenced by the amount of gas flowing downward in the dipleg, also called gas underflow. The higher the underflow, the better the solid efficiency of the cyclone.

- However, other works in the literature [48] reported that the solid flux in the cyclone dipleg promotes the gas to flow downward with the particles. In this case, the higher the solid loading and the collection efficiency, the larger the gas underflow.

Consequently, when the solid loading is increased, a compromise must be chosen between the solid and the gas collection efficiency. Optimize the cyclone solid collection efficiency is to the detriment of gas collection efficiency and vice versa.

The CFD model presented in this paper gives the opportunity to accurately predict cyclone performances. It seems therefore well-adapted for performing cyclone design optimization and troubleshooting actions in order to continuously improve technology development. Some perspectives may be related to CFD approach improvements, for example by including small scale models (i.e. particle agglomerations and interactions, drag laws modeling…) and potentially simulating the whole CFB process.

6 Acknowledgment

The authors are thankful to the FCC Alliance for very fruitful discussions and comments on this work.

7 References

[1] D. Kunii, O. Levenspiel, Fluidization Engineering : Second Edition, Elsevier, 2013.

[2] J.R. Grace, A.A. Avidan, T.M. Knowlton, Circulating fluidized beds, Blackie Academic & Professional, 1996.

[3] R. Sadeghbeigi, Fluid Catalytic Cracking Handbook, Gulf Publishing Company Houston TX, 1995.

[4] A.C Hoffmann, L.E. Stein, Gas cyclones and swirl tubes : principles, design and operation, *Springer Second Edition*, 2002.

[5] T.M. Knowlton, S.B. Karri, Differences in cyclone operation at low and high solids loading, Industrial Fluidization South Africa IFSA, Johannesburg, South Africa, 2008.

[6] C. Cortés, A. Gil, Modeling the gas and particle flow inside cyclone separators, *Progress in Energy and Combustion Science*, 33(2007), 409-452.

[7] S. Yuu, T. Jotaki, Y. Tomita, K. Yoshida, The reduction of pressure drop due to dust loading in a conventional cyclone, *Chemical Engineering Science*, 33(1978), 1573-1580.

[8] T.M. Knowlton, Cyclone systems in circulating fluidized beds, *12th International Conference on Fluidized Bed Technology CFB-12*, Krakow, Poland, May 2017.

[9] C.B. Shepherd, C.E. Lapple, Flow pattern and pressure drop in cyclone dust collectors, Industrial and Engineering Chemistry, 31(1939), 972-984.

[10] J. Casal, J.M. Martinez-Benet, A better way to calculate cyclone pressure drop, Chemical Engineering, Jan. Issue(1983), 90-99.

[11] L.W. Briggs, Effect of dust concentration on cyclone performance, Transactions of the American Institute of Chemical Engineers, 42(1946), 511-526.

[12] C.J. Stairmand, Pressure drop in cyclone separators, Engineering, 168(1949), 409-412.

[13] I. Karagoz, A. Avci, Modelling of the pressure drop in tangential inlet cyclone separators, Aerosol Science and Technology, 39(2005), 857-865.

[14] J. Chen, M. Shi, A universal model to calculate cyclone pressure drop, *Powder Technology*, 171(2007), 184-191.

[15] F.L. Fassani, L.G. Jr., A study of the effect of high inlet solids loading on a cyclone separator pressure drop and collection efficiency, Powder Technology, 107(2000), 60-65.

[16] W. Barth, Berechnung und Auslegung von Zyklonabscheidern au Grund neuerer Untersuchungen, (In German), *Brennstoff-Wärme-Kraft*, 1(1956), 1-9.

[17] E. Muschelknautz, Die Berechnung vob Zyklonabscheidern für Gase, (In German), *Chemie-Ing-Techn*, 44(1972), 63-71.

[18] J. Dirgo, D. Leith, Cyclone collection efficiency: Comparison of experimental results with theoretical predictions, *Aerosol Science and Technology*,4(1985), 401-415.

[19] J. Gimbun, T.G. Chuah, T.S. Choong, A. Fakhru'l-Razi, A CFD study on the prediction of cyclone collection efficiency, International Journal for Computational Methods in Engineering Science and Mechanics, 6(2005), 161-168.

[20] C.E. Lapple, Gravity and centrifugal separation, American Industrial Hygiene Association, 11(1950), 40-48.

[21] D. Leith, W. Licht, The collection efficiency of cyclone type particle collectors – a new theoretical approach, Air pollution and its control – AIChE Symposium Series, 68(1972), 196-206.

[22] W.H. Koch, W. Licht, New design approach boosts cyclone efficiency, Chemical Engineering, 7(1977), 80-88.

[23] A.C. Hoffmann, H. Arends, H. Sie, An experimental investigation elucidating the nature of the effect of solids loading on cyclone performance, *Filtration & Separation*, 28(1991), 188-193.

[24] R. Andreux, G. Ferschneider, M. Hémati, O. Simonin, Experimental study of a fast gas-particle separator, *Chemical Engineering Research and Design*, 58(2007), 808-814.

[25] L. Raynal, F. Augier, F. Bazer-Bachi, Y. Haroun, C. Pereira da Fonte, CFD applied to process development in the oil and gas industry – A review, Oil & Gas Science and Technology, 71(2016), 42.

[26] D. Gidaspow, Multiphase flow and fluidization : Continuum and kinetic theory descriptions, Academic Press, 1994.

[27] K. Elsayed, C. Lacor, Optimization of the cyclone separator geometry for minimum pressure drop using mathematical models and CFD simulations, *Chemical Engineering Science*, 65(2010), 6048-6058.

[28] K. Elsayed, C. Lacor, The effect of cyclone inlet dimensions on the flow pattern and performance, *Applied Mathematical Modelling*, 35(2011), 1952-1968.

[29] S.K. Shukla, P. Shukla, P. Ghosh, Evaluation of numerical schemes for dispersed phase modeling of cyclone separators, *Engineering Applications of Computational Fluid Mechanics*, 5(2011), 235-246.

[30] J.J. Derkson, S. Sundaresan, H.E.A van den Akker, Simulation of mass-loading effects in gas-solid cyclone separators, Powder Technology, 163(2006), 59-68.

[31] K.W. Chu, B. Wang, D.L. Xu, Y.X. Chen, A.B. Yu, CFD-DEM simulation of the gas-solid flow in cyclone separator, Chemical Engineering Science, 66(2011), 834-847.

[32] P. Kozołub, A. Klimanek, R.A. Bialecki, W.P. Adamczyk, Numerical simulation of a dense solid particle flow inside a cyclone separator using the hybrid Euler-Lagrange approach, Particuology, 31(2017), 170-180.

[33] M.J. Andrews, P.J. O'Rourke, The multiphase particle-in-cell (MP-PIC) method for dense particulate flows, International Journal of Multiphase Flow, 2(1996), 379-402.

[34] D.M. Snider, P.J. O'Rourke, M.J. Andrews, Sediment flow in inclined vessels calculated using a multiphase particle-in-cell model for dense particle flows, International Journal of Multiphase Flow, 24(1998), 1359-1382.

[35] D.M. Snider, An incompressible three-dimensional multiphase particle-in-cell model for dense particle flows, Journal of Computational Physics, 170(2001), 523-549.

[36] S. Kraft, F. Kirnbauer, H. Hofbauer, CPFD simulation of an industrial-sized dual fluidized bed steam gasification system of biomass with 8 MW fuel input, Applied Energy, 190(2017), 408-420.

[37] C. Chen, J. Werther, S. Heinrich, H.Y. Qi, E.U. Hartge, CPFD simulation of circulating fluidized bed risers, Powder Technology, 235(2013), 238-247.

[38] B. Amblard, R. Singh, E. Gbordzoe, L. Raynal, CFD modeling of the coke combustion in an industrial FCC regenerator, Chemical Engineering Science, 170(2017), 731-742.

[39] Y. Liang, Y. Zhang, T. Li, C. Lu, A critical validation study on CPFD model in simulating gas-solid bubbling fluidized beds, Powder Technology, 263(2014), 121-134.

[40] M. Kodam, B.J. Freireich, M.T. Pretz, B.A. Stears, Performance prediction of riser termination devices using Barracuda Virtual Reactor®, Powder Technology, 316(2017), 190-197.

[41] J.J. Derksen, Separation performance predictions of a Stairmand high-efficiency cyclone, AIChE Journal, 49(2003), 1359-1371.

[42] H. Shalaby, K. Pachler, K. Wozniak, G. Wozniak, Comparative study of the continuous phase flow in a cyclone separator using different turbulence models, International Journal for Numerical Method in Fluids, 48(2005), 1175-1197.

[43] J. Smagorinsky, General circulation experiments with the primitive equations : I. The basic experiments, Monthly weather review, 91(1963), 99-164.

[44] S.E. Harris, D.G. Crighton, Solitons, solitary waves and voidage disturbances in gas-fluidized beds, Journal of Fluid Mechanics, 266(1994), 243-276.

[45] J. Gao, X. Lan, Y. Fan, J. Chang, G. Wang, C. Lu, C. Xu, CFD modeling and validation of the turbulent fluidized bed of FCC particles, AIChE Journal, 55(2009), 1680-1694.

[46] J. Ding, D. Gidaspow, A bubbling fluidization model using kinetic theory of granular flow, *AIChE Journal*, 36(1990), 523-538.

[47] T. Gauthier, J. Bayle, P. Leroy, FCC : Fluidization phenomena and technologies, *Oil & Gas Science and Technology*, 55(2000), 187-207.

[48] R. Karri, T. Knowlton, Streaming flow in cyclone diplegs, *Fluidization X Conference*, May 20-24, 2001, Beijing, China.